

both excess Gibbs free energy and heat of mixing data for a binary mixture, from which binary parameters must be determined, to interpolate or extrapolate these thermodynamic quantities. Ternary heat of mixing data is successfully predicted by using the component parameters determined from binary data regardless of the equation used.

Acknowledgment

The authors thank the Data Processing Center, Kyoto University, and the Computation Center, Kanazawa University, for the use of their facilities.

Nomenclature

C_1, C_2	= values of $(g_{21} - g_{11})$ and $(g_{12} - g_{22})$ at 0°C, cal/mol
C_3	= value of α_{12} at 0°C
D_1, D_2	= coefficients of temperature change of $(g_{21} - g_{11})$ and $(g_{12} - g_{22})$, cal/mol °C
D_3	= coefficient of temperature change of α_{12} , °C ⁻¹
g^E	= excess Gibbs free energy, cal/mol
g_{ij}	= energies of interaction between an $i - j$ pair of molecules, cal/mol
G_{ij}	= coefficient as defined by $G_{ij} = \rho_{ij} \exp(-\alpha_{12}\tau_{ij})$
h^E	= excess enthalpy of mixing, cal/mol
P	= total pressure, atm
P_i^s	= saturated vapor pressure of pure component i at system temperature, atm
p	= coefficient (0 or 1) of Equations 1, 2, 3, and 5
q	= coefficient (0 or 1) of Equations 1, 2, 3, and 5
R	= gas constant, 1.987 cal/mol °K
T	= absolute temperature, °K
x_i	= liquid phase mole fraction of component i
y_i	= vapor phase mole fraction of component i
v_i	= molar volume of pure liquid i , cc/mol

GREEK LETTERS

α_{12}	= nonrandomness constant for binary 1-2 interaction
γ_i	= activity coefficient of component i in the liquid phase
ϕ_i	= fugacity coefficient for component i in the vapor phase
ϕ_i^s	= fugacity coefficient for pure saturated vapor i at system temperature and p_i^s

τ_{ij} = coefficient as defined by $\tau_{ij} = (g_{ij} - g_{jj})/RT$
 ρ_{ij} = coefficient as defined by $G_{ij} = \rho_{ij} \exp(-\alpha_{12}\tau_{ij})$

SUBSCRIPT

i = component

SUBSCRIPTS

E = excess

s = saturated

Literature Cited

- Asselineau, L., Renon, H., *Chem. Eng. Sci.*, **25**, 1211 (1970).
 Bekarek, V., *Collect. Czech. Chem. Commun.*, **33**, 2608 (1968).
 Brown, I., Smith, F., *Aust. J. Chem.*, **7**, 264 (1954).
 Duran, J. L., Kaliaguine, S., *Can. J. Chem. Eng.*, **49** (4), 278 (1971).
 Hanks, R. W., Gupta, A. C., Christensen, J. J., *Ind. Eng. Chem. Fundam.*, **10**, 504 (1971).
 Hirobe, H., *J. Sci. Tokyo*, **1**, 155 (1926).
 Kaliaguine, S., Ramalho, R. S., *Can. J. Chem. Eng.*, **50** (1), 139 (1972).
 Kudryavtseva, L. S., Susarev, M. P., *Zh. Prikl. Khim.* **36**, 1231 (1963a).
 Kudryavtseva, L. S., Susarev, M. P., *ibid.*, **1963b**, p 1471.
 Mrazek, R. V., Van Ness, H. C., *AIChE J.*, **7**, 190 (1961).
 Nagata, I., 10th Symposium Chem. Eng. Soc., Nagoya, Japan, November 1971.
 Nagata, I., Ohta, T., *Kagaku Kogaku*, **33**, 263 (1969).
 Nelder, J. A., Mead, R., *Computer J.*, **7**, 308 (1965).
 O'Connell, J. P., Prausnitz, J. M., *Ind. Eng. Chem. Process Des. Develop.*, **6**, 245 (1967).
 Orye, R. V., PhD dissertation, University of California, Berkeley, Calif., 1965.
 Renon, H., PhD dissertation, University of California, Berkeley, Calif., 1966.
 Renon, H., Asselineau, L., Cohen, G., Rambault, C., "Calcul sur Ordinateur des Équilibres Liquide-Vapeur et Liquide-Liquide," pp 168, 169, Éditions Technip, Paris, France, 1971.
 Renon, H., Prausnitz, J. M., *AIChE J.*, **14**, 135 (1968).

RECEIVED for review March 6, 1972

ACCEPTED May 9, 1972

Tables II-V and Literature Cited for these tables will appear following these pages in the microfilm edition of this volume of the Journal. Single copies may be obtained from the Business Operations Office, Books and Journals Division, American Chemical Society, 1155 Sixteenth St., N.W., Washington, D.C. 20036. Refer to the following code number: PROC-72-574. Remit by check or money order \$3.00 for photocopy or \$2.00 for microfiche.

Fractionation Efficiency

Eighteen-Inch Valve Tray Column

William G. Todd and Mathew Van Winkle¹

University of Texas, Chemical Engineering Department, Austin, Tex. 78712

Because distillation is a very important industrial process for separating chemical components by physical means, much effort has been expended to increase the performance of existing distillation equipment and to develop new types of vapor-liquid contacting devices which more closely attain equilibrium (the condition of 100% efficiency) between the distilling phases. Equilibrium conditions are rarely achieved in actual operating equipment and the separation efficiency of the particular device must be evaluated to describe quanti-

tatively the relative approach to equilibrium that is obtained between the phases. Even the most detailed tray calculations must rely on such a predicted efficiency for the determination of the actual number of trays required.

The success of valve trays as vapor-liquid contactors has made it necessary to develop an efficiency prediction method for these contactors. Although various efficiency and hydraulic data have been reported for valve trays in literature, there does not exist a generalized efficiency prediction correlation for these trays.

The relative approach to equilibrium obtained by a con-

¹ To whom correspondence should be addressed.

The purpose of this study was to collect experimental tray efficiency data. The experimental work was conducted in an 18-in. diameter distillation column containing three valve trays of the rectangular type. A Box-Behnken experimental design was used to investigate the effects on tray efficiency of tray valve leg lengths, tray outlet weir heights, internal column molal liquid to vapor ratios, and the internal column loadings expressed as percents of the column flooding point. The *n*-propanol-toluene binary system and the benzene-*n*-propanol binary system were investigated. Valve tray pressure drops, clear liquid depths, froth heights, efficiency, and flooding capacities are reported for 116 cases.

tacting device depends upon the rate of mass transfer between the phases, which in turn is a complicated function of the mass and heat transfer coefficients, the relative temperature and concentration gradients in the liquid and vapor phases, the length of contact time, and amount of contact area between the phases. To investigate the effects of these various physical properties and operating variables on the mass transfer between the distilling phases, a study was undertaken with an 18-in. diameter distillation column containing three valve trays. The valves were the rectangular type. This particular column diameter was selected so that the wall effects predominant in smaller diameter columns would be diminished.

The purpose of this article, the first of two articles, is to define the scope of the study undertaken, to describe the equipment and procedures utilized, and to present the experimental column flooding points, average tray froth heights, equivalent tray clear liquid depths, tray pressure drops, and tray efficiencies. The second article will present developed correlations for predicting valve tray froth heights, clear liquid depths, and efficiencies using the existing and proposed theories of mass transfer and separation efficiency.

Scope of Work

To study the effects of tray hydraulics, phase residence times, and mass and heat transfer on valve tray efficiencies under distilling conditions, a Box-Behnken response-surface experimental design (Box, 1960), which employs a subset of the points in a full three-level factorial, was used. This type of design was selected to maximize the benefits of experimentation while minimizing the number of data points. This in turn minimized the high utility usage (maximum heat exchange of 1.0 million Btu/hr) required for the operation of the distillation unit.

The independent variables of the experimental design were the tray valve leg lengths (equivalent to varying the tray hole area), the tray outlet weir heights, the internal column molal liquid to vapor (*L/V*) ratio, internal column loadings expressed as percents of the column flooding point, and the physical properties of the operating system. With the exception of the physical properties, three different values of each of the independent variables were investigated. Two different binary systems (*n*-propanol-toluene and benzene-*n*-propanol) were selected to represent the physical properties of interest, namely the ratio of the molal latent heats of vaporization and the surface tension of the components. Tables I and II contain, respectively, the numerical values for the different design levels and the coded Box-Behnken design for four variables. The 27 experimental data points designated in Table II were performed for each of the two binary systems, giving a total of 54 data sets.

These experimental variables were selected with the expectation of gaining further insight into the dependence on these variables of the tray clear liquid depth, the tray froth height, the total interfacial contact area, the residence times,

Table I. Experiment Design Levels

Variable	Levels		
	-1	0	+1
X1 Tray valve leg length, in.	0.3125	0.3750	0.4375
X2 Tray weir height, in.	1	2	3
X3 <i>L/V</i> ratio	0.5	1.0	1.5
X4 % of flood	30	60	90

Table II. Coded Four-Variable Box-Behnken Design

X1	X2	X3	X4
+1	+1	0	0
+1	-1	0	0
-1	+1	0	0
-1	-1	0	0
0	0	+1	+1
0	0	+1	-1
0	0	-1	+1
0	0	-1	-1
0	0	0	0
+1	0	0	+1
+1	0	0	-1
-1	0	0	+1
-1	0	0	-1
0	+1	+1	0
0	+1	-1	0
0	-1	+1	0
0	-1	-1	0
0	0	0	0
+1	0	+1	0
+1	0	-1	0
-1	0	+1	0
-1	0	-1	0
0	+1	0	+1
0	+1	0	-1
0	-1	0	+1
0	-1	0	-1
0	0	0	0

contact times, and the mass transfer between phases, thus providing a basis for correlating the valve tray efficiencies. Because of the apparent dependence of the contact areas and residence times on the froth height, the photographic technique developed by Flint (1965) for accurately measuring tray froth heights was used.

In addition to the 54 design data sets, supplementary data were collected at the 15, 30, 45, 60, 75, 90, and 97.5% of the column flooding conditions for both binaries at each length of tray valve legs. The tray weir height and *L/V* ratio were held constant at the coded 0 level for these runs. These additional points of data were taken to gain a better understanding of the operations of valve trays over a wide range of column loadings. This series of runs also allowed a subjective

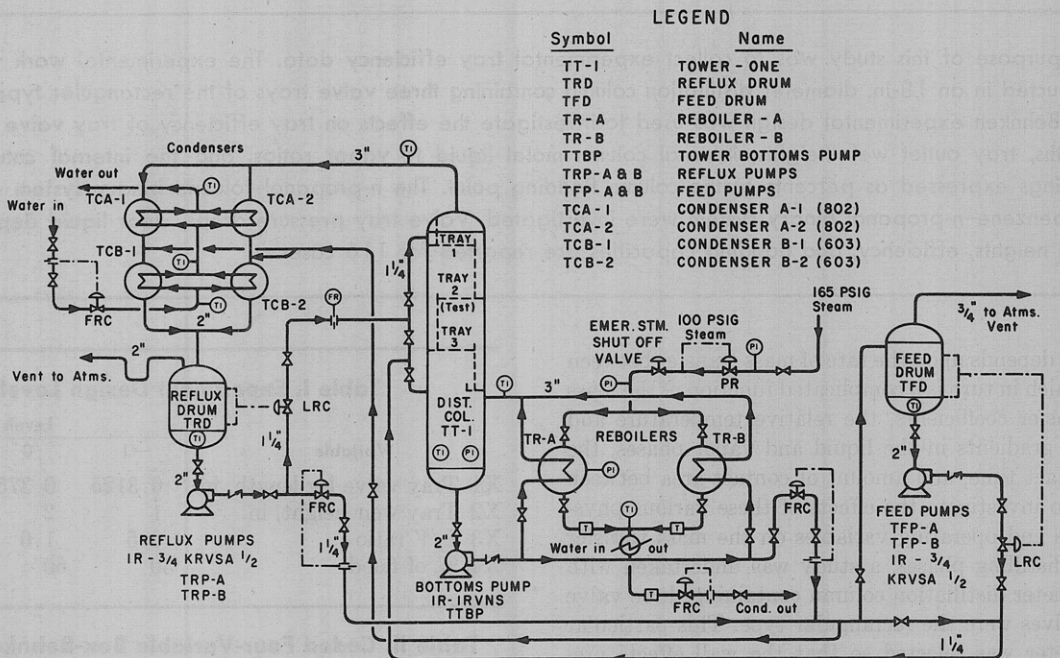


Figure 1. Process flow sheet

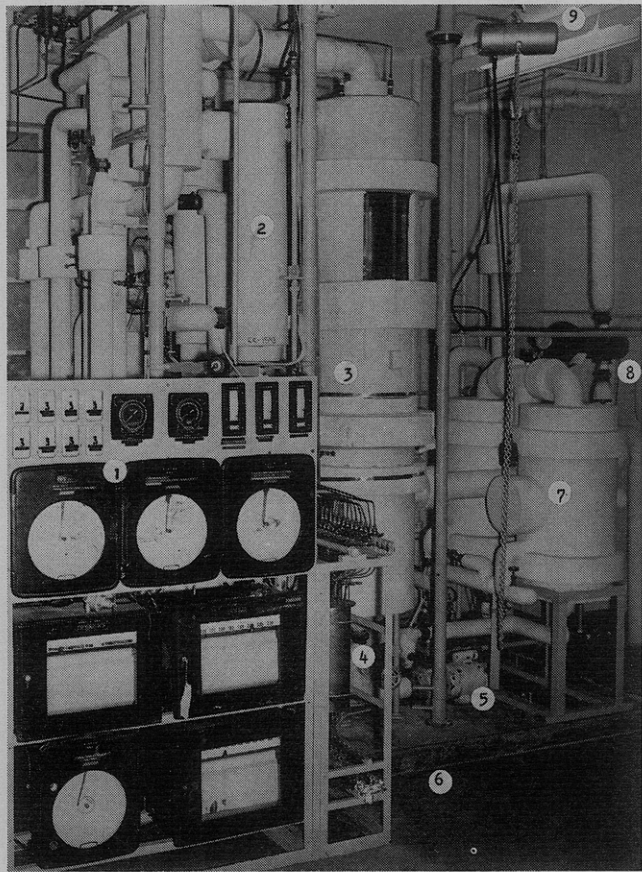


Figure 2. Distillation unit

determination of the amount of tray weeping and entrainment.

Experimental Apparatus

Figures 1 and 2, respectively, are the process flow sheet and a photograph of the 18-in. diameter distillation column and related equipment. Two 18 × 24-in. glass sections of

the column permitted visual observation of the tray action. The stainless steel valve tray assembly was a standard 18-in. diameter package featuring adjustable weir heights and adjustable downcomer escape clearances. Three different sets of interchangeable valves were also available. Figure 3 is a photograph showing one of the glass sections being lifted from the valve tray package. The pertinent data of the tray package and distillation column are listed in Table III.

The instrumentation used in control of the distillation column was pneumatic, and the various flow rates were measured by orifice meters. Two multipoint temperature recorders using copper-constantan and iron-constantan thermocouples were employed to monitor the temperatures of 24 different points within the distillation unit.

All differential pressures were measured by pneumatic differential pressure cell transmitters. The equivalent clear liquid head (or hydraulic liquid head) reported in the study was defined as the pressure drop in terms of clear liquid across the two-phase vapor-liquid bed on tray 2. All pressure sensing lead lines were continuously purged with nitrogen to ensure no buildup of vapor, condensed vapor, or liquid.

Thirteen different samples were taken for each point of data. These consisted of three vapor samples above tray 2, three vapor samples above tray 3, two liquid samples from tray 2, liquid samples from the downcomers of trays 1, 2, and 3, bottom and overhead products. All samples were collected downstream of a sample cooler. A precision refractometer was used for analysis of sample compositions by determining the refractive index at 25°C.

Because of the potential danger inherent in operating a distillation unit within a closed laboratory, certain safety equipment was installed as an integral part of the experimental apparatus. The various pieces of safety equipment provided were an exhaust fan, an emergency steam shutoff valve, emergency electrical cutoff switch, a dike enclosing the distillation unit, a positive nitrogen purge on the system, and numerous carbon dioxide extinguishers.

Experimental Procedure

Each point of data collected was designated with a three-

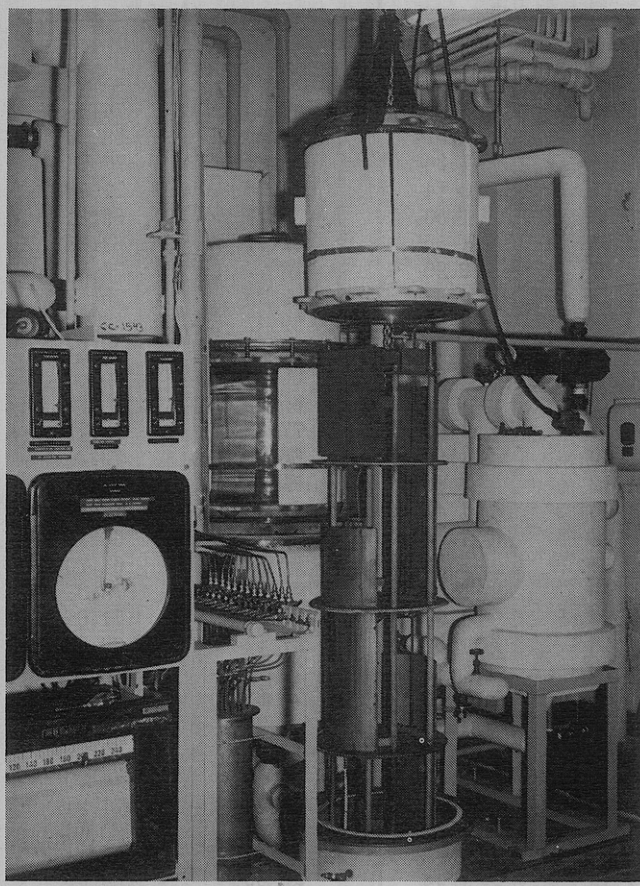


Figure 3. Valve tray assembly

character run number. The first character of the run number denoted which binary system was being studied (1 denotes the *n*-propanol-toluene binary system and 2 denotes the benzene-*n*-propanol system) and the last two characters of the run number denoted the values of the independent variables (Table IV). The supplementary data were denoted with run numbers which contained an alphabetic character in the second position (A and F sets—value leg lengths of 0.4375; B and E sets—value leg lengths of 0.3750; C and D sets—value leg lengths of 0.3125). Runs A, B, and C were with the *n*-propanol-toluene binary and D, E, and F were with the benzene-*n*-propanol binary.

Since the percent of flood was one of the operating variables, the column flood point had to be experimentally determined for each combination of independent variables. To determine the column flood point for a particular set of conditions, the unit was started up and the reboiler steam rate was incrementally increased until a positive indication of flooding occurred. This indication was normally a sudden and large increase in reflux rate for a small increase in steam rate. The magnitude of this increase in the reflux rate was such that the reflux drum level would increase at such a rate to be out of control. The liquid level in the bottom of the column would fall rapidly, and the column bottom pressure would rise and start fluctuating. At this point the bed froth heights on the trays were equivalent to the tray spacings.

The steam flow at the flood point was measured by collecting the steam condensate in a 55-gal. drum for a measured time interval. The weight of the drum was recorded before and after the collection period and the weight average flow rate was computed. This procedure was used to measure the steam flow for all experimental data points.

Table III. Valve Tray Specifications

Minimum tower cross-sectional area, ^a ft ²	1.68
Number of trays	3
Tray spacing, ^b in.	18.0
Active or bubbling area per tray, ft ²	1.06
Net area per tray, ft ²	1.45
Number of valves per tray	16.0
Number of rows of valves per tray	3.0
Segmental downcomer area, top and bottom, ft ²	0.102
Adjustable weir height, in.	1.0 4.0
Weir heights used in this study, in.	1.0 2.0 3.0
Adjustable downcomer escape clearance, in.	0.75 2.0
Downcomer escape clearance used in this study, in.	0.75
Weir length, in.	8.875
Valve leg lengths ^c used in this study, in.	0.3125 0.3750 0.4375
Slot area ^d (% Active area) for 0.3125-in. valves	10.87
Slot area (% Active area) for 0.3750-in. valves	12.50
Slot area (% Active area) for 0.4375-in. valves	15.50

^a Based upon a minimum inside column diameter of 17-17/32-in. ^b The tray spacing above the first tray was 15-in. ^c Valve leg length = maximum lift of the valve plus the thickness of the tray deck. ^d Slot area =

$$\frac{(2)(100)(N)(\text{lift of valve})(\text{length of the valve slot})}{(144)A_a}$$

where

$$N = \text{number of valves per tray}$$

$$A_a = \text{active or bubbling area per tray}$$

Table IV. Experimental Run Numbers and Level of Variables

Run ^a no.	Valve leg length	Weir height	L/V	% Flood
01	0.4375	3	1	60
02	0.4375	1	1	60
03	0.4375	2	1	30
04	0.4375	2	1	90
05	0.4375	2	1.5	60
06	0.4375	2	0.5	60
07	0.3750	2	1.5	90
08	0.3750	2	1.5	30
09	0.3750	2	0.5	90
10	0.3750	2	0.5	30
11	0.3750	2	1	60
12	0.3750	2	1	60
13	0.3750	3	1.5	60
14	0.3750	3	0.5	60
15	0.3750	3	1	90
16	0.3750	3	1	30
17	0.3750	1	1.5	60
18	0.3750	1	0.5	60
19	0.3750	1	1	90
20	0.3750	1	1	30
21	0.3750	2	1	60
22	0.3125	2	1	30
23	0.3125	2	1	90
24	0.3125	2	1.5	60
25	0.3125	2	0.5	60
26	0.3125	3	1	60
27	0.3125	1	1	60

^a Last two characters of a run number.

Table V. Experimental Results

Run code	F_s	% Flood	Z_f	Z_c	ΔP_T	E_{MV^c}	E_{MV^o}
101	0.88	58.10	7.53	0.95	1.50	67.35	74.30
102	0.90	59.32	7.23	0.70	1.32	68.99	68.96
103	0.46	29.64	1.12	1.25	1.36	78.21	77.88
104	1.41	90.00	15.64	1.15	3.14	74.42	71.58
105	0.88	56.76	7.91	1.03	1.53	70.57	69.31
106	1.02	61.91	8.94	0.55	1.55	62.61	63.66
107	1.28	91.02	13.10	1.12	2.90	73.77	73.39
108	0.44	28.27	5.23	1.32	1.32	82.20	76.88
109	1.47	89.83	15.59	0.88	2.86	59.47	63.59
110	0.44	28.30	4.95	0.90	1.15	43.00	65.31
111	0.96	60.70	8.40	0.65	1.60	66.94	69.60
112	0.95	60.79	7.96	0.75	1.55	65.48	69.30
113	0.85	60.02	8.16	0.87	1.57	77.62	72.27
114	0.98	60.01	8.20	0.60	1.60	68.23	72.30
115	1.39	90.55	15.97	1.12	3.26	71.77	73.48
116	0.43	27.74	5.58	1.30	1.47	81.12	76.18
117	0.89	62.30	7.74	0.78	1.44	64.83	66.16
118	1.02	61.60	9.88	0.34	1.45	60.34	64.70
119	1.40	91.55	16.28	0.80	2.84	68.69	73.07
120	0.47	30.27	4.84	0.80	1.02	70.76	71.02
121	0.97	61.52	8.30	0.58	1.55	67.17	69.93
122	0.48	29.71	5.51	1.25	1.35	76.90	76.93
123	1.43	91.13	15.53	1.31	3.00	70.62	73.52
124	0.95	62.50	8.56	0.80	1.86	72.72	76.10
125	1.11	61.50	10.47	0.68	1.98	74.15	72.27
126	1.01	62.62	9.30	0.80	2.05	68.99	74.90
127	1.00	62.37	9.37	0.63	1.76	64.43	71.94
201	1.04	60.55	10.23	1.13	1.62	59.11	60.14
202	1.04	60.11	10.56	0.93	1.45	50.24	55.15
203	0.53	29.64	6.11	1.45	1.42	64.38	62.78
204	1.51	89.46	16.33	1.13	3.25	56.30	53.60
205	0.95	61.25	9.08	1.10	1.50	59.86	59.32
206	1.04	60.80	10.93	0.75	1.40	53.26	51.09
207	1.36	90.50	15.05	1.37	3.25	64.93	51.65
208	0.50	31.62	5.84	1.50	1.47	64.93	67.09
209	1.47	89.56	16.29	0.96	3.08	73.27	44.08
210	0.52	30.00	5.63	1.15	1.30	48.64	57.39
211	1.04	59.22	9.74	0.87	1.72	55.33	58.49
212	1.03	59.44	9.45	0.80	1.72	55.47	58.24
213	0.95	59.86	9.83	1.13	1.79	63.18	62.23
214	1.05	60.90	10.69	0.60	1.70	90.80	57.75
215	1.51	90.04	16.69	1.23	3.88	57.62	54.71
216	0.54	30.43	6.06	1.45	1.50	62.46	66.76
217	0.95	59.86	8.71	0.88	1.55	56.19	58.05
218	1.05	60.90	11.10	0.45	1.61	51.69	50.13
219	1.51	89.48	15.82	1.10	3.10	53.31	55.77
220	0.54	30.43	6.67	1.15	1.21	56.97	60.17
221	1.05	59.78	9.77	0.80	1.75	56.55	60.17
222	0.54	30.26	6.03	1.30	1.39	63.59	63.95
223	1.49	89.80	16.63	1.13	3.44	57.23	54.71
224	0.96	61.88	8.56	0.87	1.81	63.22	61.71
225	1.03	60.00	11.20	0.60	1.81	63.76	53.13
226	1.03	59.78	9.77	0.80	1.91	60.60	63.49
227	1.03	59.56	10.39	0.62	1.75	51.94	58.25
1A1	0.23	15.01	^a	1.00	0.96	80.81	78.08
1A2	0.46	29.64	5.30	1.25	1.36	78.21	77.88
1A3	0.71	44.92	^a	0.92	1.31	71.34	74.42
1A4	0.94	60.35	7.56	0.88	1.46	67.67	69.49
1A5	1.18	75.68	10.39	0.70	2.05	68.40	67.59
1A6	1.41	90.00	15.64	1.15	3.14	74.42	71.58
1A7	1.52	97.25	18.00	1.40	3.75	68.04	70.38
1B1	0.26	16.78	3.69	1.20	1.00	78.88	75.11
1B2	0.52	32.22	5.30	1.22	1.40	75.87	75.34
1B3	0.71	44.25	6.23	0.90	1.32	68.25	70.62
1B4	0.96	60.70	8.40	0.65	1.60	66.94	69.60
1B5	1.17	75.17	10.86	0.70	2.12	65.27	69.58
1B6	1.39	90.81	15.55	1.00	2.98	69.80	72.92
1B7	1.48	97.25	18.00	1.40	3.85	70.32	71.22

Table V. (Continued)

Run code	F_s	% Flood	Z_f	Z_c	ΔP_T	E_{MV^c}	$\overline{E_{MV^c}}$
1C1	0.22	13.66	3.35	1.00	0.95	73.60	76.61
1C2	0.48	29.71	5.51	1.25	1.35	76.90	76.60
1C3	0.74	45.55	6.86	0.94	1.10	68.92	72.25
1C4	1.00	62.37	9.12	0.85	1.60	68.22	72.13
1C5	1.23	76.97	11.30	0.93	2.30	68.03	71.95
1C6	1.43	91.13	15.53	1.31	3.00	70.62	73.52
1C7	1.48	94.45	18.00	1.55	3.88	68.87	72.42
2D1	0.27	15.00	3.85	1.15	1.00	61.30	62.07
2D2	0.54	30.46	6.65	1.25	1.27	62.60	64.49
2D3	0.81	45.33	7.67	0.97	1.52	59.10	62.05
2D4	1.05	60.68	9.56	0.90	2.12	59.47	59.69
2D5	1.26	75.52	12.31	0.82	2.55	55.75	58.47
2D6	1.44	88.64	18.00	1.15	3.40	62.21	57.18
2D7	1.57	97.78	18.00	1.40	3.82	54.70	53.59
2D1	0.23	13.04	3.48	1.10	0.98	59.59	62.40
2D2	0.54	30.26	6.03	1.30	1.39	63.59	63.95
2D3	0.81	45.84	7.54	1.00	1.42	59.25	60.21
2D4	1.07	61.29	9.76	0.75	2.00	56.89	61.07
2D5	1.30	75.85	14.22	0.80	2.50	55.09	58.82
2D6	1.49	89.80	16.63	1.13	3.44	57.23	54.71
2D7	1.54	96.89	18.00	1.30	3.75	49.67	52.49
2E1	0.24	13.11	3.63	1.27	1.09	61.71	62.02
2E2	0.52	29.22	6.03	1.40	1.42	63.41	65.31
2E3	0.80	45.33	7.29	0.98	1.40	55.51	60.54
2E4	1.04	59.22	9.74	0.87	1.72	55.33	58.49
2E5	1.26	72.93	12.31	0.88	2.38	55.96	57.13
2E6	1.51	91.05	16.42	1.07	3.10	56.59	54.50
2E7	1.58	96.44	18.00	1.30	3.65	59.87	49.74
2E1	0.26	15.18	^a	1.37	1.08	56.34	61.08
2E2	0.53	29.64	^a	1.35	1.44	63.76	64.27
2E3	0.79	44.44	^a	1.05	1.40	57.23	60.85
2E5	1.29	74.59	^a	0.88	2.38	57.24	58.19
2E6	1.49	88.89	^a	1.07	3.13	54.85	56.74
2E7	1.61	97.56	^a	1.30	3.75	58.20	50.73
2F1	0.27	14.89	3.77	1.38	1.07	60.30	61.85
2F2	0.53	29.64	6.11	1.45	1.42	64.38	62.78
2F3	0.81	45.44	7.87	0.95	1.35	58.88	59.20
2F4	1.06	60.44	10.11	0.75	1.55	54.75	57.71
2F5	1.30	75.44	12.64	0.80	2.08	53.31	55.96
2F6	1.51	89.46	16.33	1.13	3.25	56.30	53.60
2F7	1.58	96.61	18.00	1.25	3.25	58.16	50.59
2F1	0.26	14.96	^a	1.25	1.07	58.74	61.54
2F2	0.54	30.17	^a	1.50	1.42	65.62	62.25
2F3	0.80	45.56	^a	1.00	1.37	58.81	59.29
2F4	1.05	60.89	^a	0.90	1.62	56.73	57.86
2F5	1.27	75.57	^a	0.80	1.97	54.44	55.96
2F6	1.48	90.56	^a	1.13	2.78	56.76	53.99
2F7	1.59	97.22	^a	1.50	3.15	56.19	52.43

^a Froth heights not reported.

Once the column flood point was determined, the set point of the steam condensate flow controller was adjusted until the recorded steam condensate flow was at the correct value (30, 60, or 90% of the flooding value). If the L/V ratio was other than unity, the amount of the respective product to be withdrawn was computed and the product flow controller adjusted to this value.

After the various operating variables were set, the unit was allowed to reach steady-state conditions. This required 45 min to 2 hr, depending upon the particular operation being performed. The general criteria for determining steady-state unit operations was a constant level in the reflux drum and a constant temperature profile throughout the distillation column. After these conditions were met for approximately 15 min, the data were collected. During the lineout time, the

steam condensate was measured as previously described and the sample lines were purged with nitrogen.

A series of five photographs of the bubbling action on tray 2 were taken at 1-min intervals. The temperatures, pressures, pressure drops, and liquid levels were recorded, and the condensed vapor and liquid samples were collected in 15-cc vials. The condensed vapor samples, collected first, were taken from the top of the column downward and the liquid samples, from the bottom tray upward. This order of sampling was recommended by Ellis (1960).

Before each sample was collected, the sample liquid was continuously withdrawn and discarded until the sample inlet to the cooler became warm, thus ensuring a representative sample. Normally, about 30 cc of sample were discarded before the sample (approximately 8 cc in volume) was col-

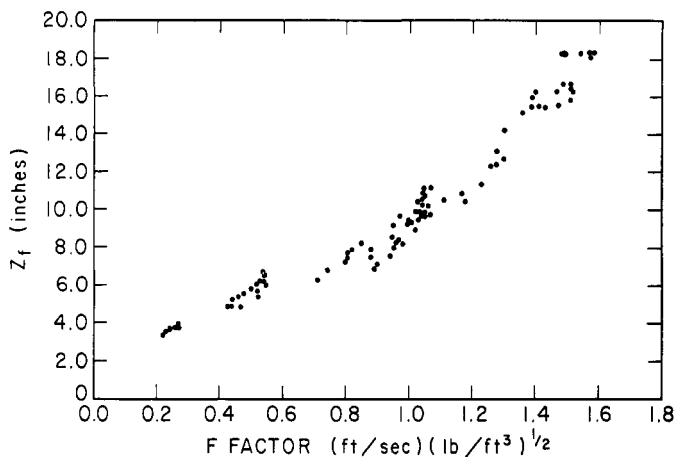


Figure 4. Froth heights (*n*-propanol-toluene and benzene-*n*-propanol systems)

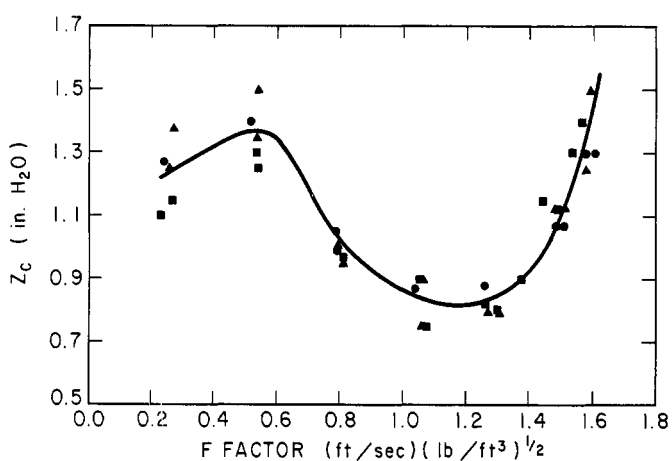


Figure 5. Clear liquid depths

D ▀, E ●, and F ▲ data sets

lected. The sample vials were immediately sealed and after all the samples were collected (4–5 min elapsed time), the individual samples were analyzed by using the refractometer.

After the samples were analyzed, the data were briefly examined for abnormalities and the unit recorders checked to ensure that steady-state operations had been maintained throughout the data collection period. If all was well, the flow rates were adjusted for the next data point.

The above procedure was repeated until all the data for the particular tray weir height had been collected. The unit was then temporarily shut down and the tray weir heights adjusted to the next height. The column flood point was redetermined and the data for this new weir height were collected. This sequence of steps was repeated until all the data had been collected for the given tray valve height. The column was then disassembled and the next set of tray valves installed. The distillation column was thoroughly purged with carbon dioxide after each disassembly to remove all traces of air.

Experimental Results

A summary of the experimental results is contained in Table V. The computed superficial F_s -factor (F_s), percent of column flood, average tray froth height (Z_f), tray clear liquid

depth (Z_c), tray pressure drop (ΔP_T), and the computed Murphree overall tray efficiency (E_{MV}^c) are reported for the test tray (the second tray). The average Murphree efficiency for the three trays is reported also (\bar{E}_{MV}^c).

The internal column flow rates and other flow factors reported in Table V and Figure 9 were computed by making enthalpy and material balance calculations around the bottom of the distillation column. (See the Appendix for details of these calculations and a sample printout of the computed results.) The vapor and liquid compositions used to compute the Murphree overall tray efficiencies were corrected for possible vaporization of liquid inside the downcomers and condensation of vapor on the outside walls of the downcomer as recommended by Ellis and Shelton (1960). They found that significant amounts of heat could be conducted through the walls of the downcomer owing to the temperature gradient between the liquid inside the downcomer and the vapor contacting the outside of the downcomer. Lowry (1967) observed similar effects. The corrections outlined in the appendix are based upon theoretical reasoning and practical engineering judgment. In general, this correction is relatively unimportant in larger sized columns because the amount of downcomer surface area is small in comparison to the total tray surface area. The vapor-liquid equilibrium data used in the efficiency computations were obtained from the following sources: *n*-propanol-toluene data reported by Lu (1957); benzene-*n*-propanol data reported by Prabhu and Van Winkle (1963).

Discussion

Column Flood Points. The experimentally determined column flood points were independent of system physical properties, valve leg lengths, and the outlet weir heights. The average F_s value which resulted in column flooding for these variables was 1.62. Increasing the internal L/V ratio was found to decrease the capacity of the distillation column. At the coded design level of 1.5 L/V , the column-flooding F_s value was 1.53 and at the coded level of 0.5 L/V , the F_s value was 1.69.

Average Tray Froth Height. From the visual observations of this study, the valve tray beds could be characterized by the liquid-dispersed type of bed as described by Sawistowski (1959) and later by Lowry (1967). The only exception to this was at the very low flow rates (15% of column flood) where the bed was quite tranquil and was characterized by bubbles of vapor dispersed in a liquid bed. No difference could be detected between the tray beds for the two different binary systems studied. The average tray bed heights are illustrated in Figure 4 as a function of the F_s -factor. No significant differences in the tray bed heights could be detected for the different values of weir heights, valve leg lengths, and L/V ratio.

Tray Clear Liquid Depth. Preliminary examination of the data indicated, with the exception of the valve leg lengths, that the tray clear liquid depth was effected by all the experimental independent variables. Figure 5 illustrates the tray clear liquid depths vs. the F_s -factor for the D, E, and F data sets and provides a better understanding of the tray bed hydraulics over the entire operating range of the valve tray. The continuous line plotted in Figure 5 is a hand-fitted curve and is included to illustrate the general shape of the plotted data. This is true for all the continuous lines plotted in this article. As discussed in the preceding paragraph, the tray bed at low flow rates is composed primarily of bubbles of vapor dispersed in a liquid bed. This

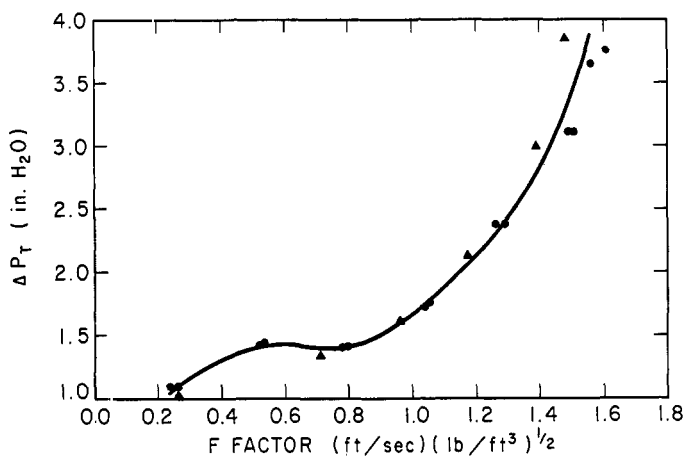


Figure 6. Valve tray pressure drops

B ▲ and E ● data sets

type of bed results in high values of the clear liquid (Figure 5).

As the vapor flow rate is increased, the tray bed is lifted from the floor by the vapor stream entering the tray and consists primarily of liquid drops suspended in the vapor stream. As the result of this increased aeration of the bed, the quantity of liquid in the bed decreases as is evident in Figure 5 at values of the F_s -factor around 1.0. As the vapor flow is increased further, the bed height increases rapidly (Figure 4), and thus the amount of total liquid holdup increases proportionally. See Figure 5. The authors reported similar bed characteristics for jet trays in a previous study (Todd, 1967).

The clear liquid depths reported for the other types of trays (A.I.Ch.E., 1958; Finch, 1964) do not demonstrate the minimum shown in Figure 5, but are more closely represented by the first half of the curve. Increasing the weir heights and the internal L/V ratios increases the depth of clear liquid on the tray. Similar results have been reported for other types of trays (A.I.Ch.E., 1958; Finch, 1964). No effect of the tray valve leg lengths on the clear liquid depth could be detected.

Tray Pressure Drop. Figure 6 is a plot of the tray pressure drop data vs. the F_s -factor for the B and E data sets and is representative of the other sets of data. The flat profile of the curve at the lower flow rates reflects the effect of the decreasing depth of clear liquid on the tray as discussed above.

Tray Efficiencies. Examination of the tabulated efficiency data indicates that the efficiencies for the *n*-propanol-toluene system are higher than those for the benzene-*n*-propanol system. This is better illustrated by the test tray efficiencies for the B data set and the E data set (Figure 7).

To illustrate the effects of the various independent operating variables on the average column efficiency, selected data for the benzene-*n*-propanol system are plotted in Figure 8. The curved line plotted in Figure 8 represents the average column efficiency for the duplicate E data sets, and the other points represent the data points in Table V labeled 207-10 and 213-20.

The general shape of the curve is in agreement with other reported data for valve trays (Dale, 1962; F.R.I., 1964; Koch, 1958) and subjectively illustrates the effect of tray weepage and entrainment on the performance of the distillation col-

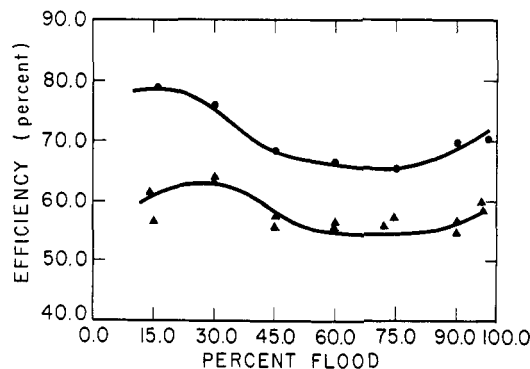


Figure 7. Test tray efficiencies

● n-Propanol-toluene B data set ▲ Benzene-*n*-propanol E data set

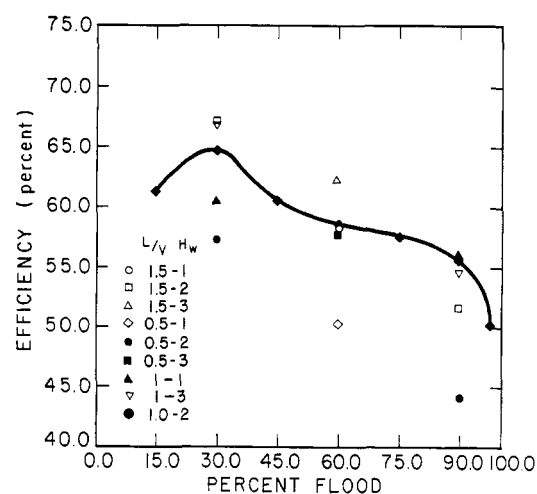


Figure 8. Average column efficiencies, benzene-*n*-propanol system

umn. At the low flow rates (15% of the column flood) the column efficiency shows a decline which could be attributed to tray weepage, but a surprisingly small amount of weepage was actually observed at this flow rate. A more likely reason for this decline in column efficiency is the type of bed (bubbles of vapor dispersed in a liquid bed) that exists at the low flow rates. This type of bed possibly results in a low effective contact area between the contacting liquid and vapor phases which, in turn, limits the mass transfer.

The effect of liquid entrainment on the column efficiency is very apparent at the high flow rates (97% of column flood) where the efficiency declines sharply owing to the excessive amount of liquid carry over. The efficiency profiles for the test tray were generally flatter than those for the column average and normally did not decline as rapidly at the 97% flood points.

Examination of the experimental design data points plotted in Figure 8 leads to the following observations: Increasing weir heights increases the average column Murphree tray efficiency at low flow rates but has little effect if any at the high flow rates. This result at the lower flow rates is in agreement with the following investigations (A.I.Ch.E., 1958; Finch, 1964; Gerster, 1951; Hellums, 1958; Umholtz, 1957). Kocatas (1962) found no effect of weir height upon overall column efficiency at high vapor rates in agreement with this work. Increasing the internal L/V ratio increases the average

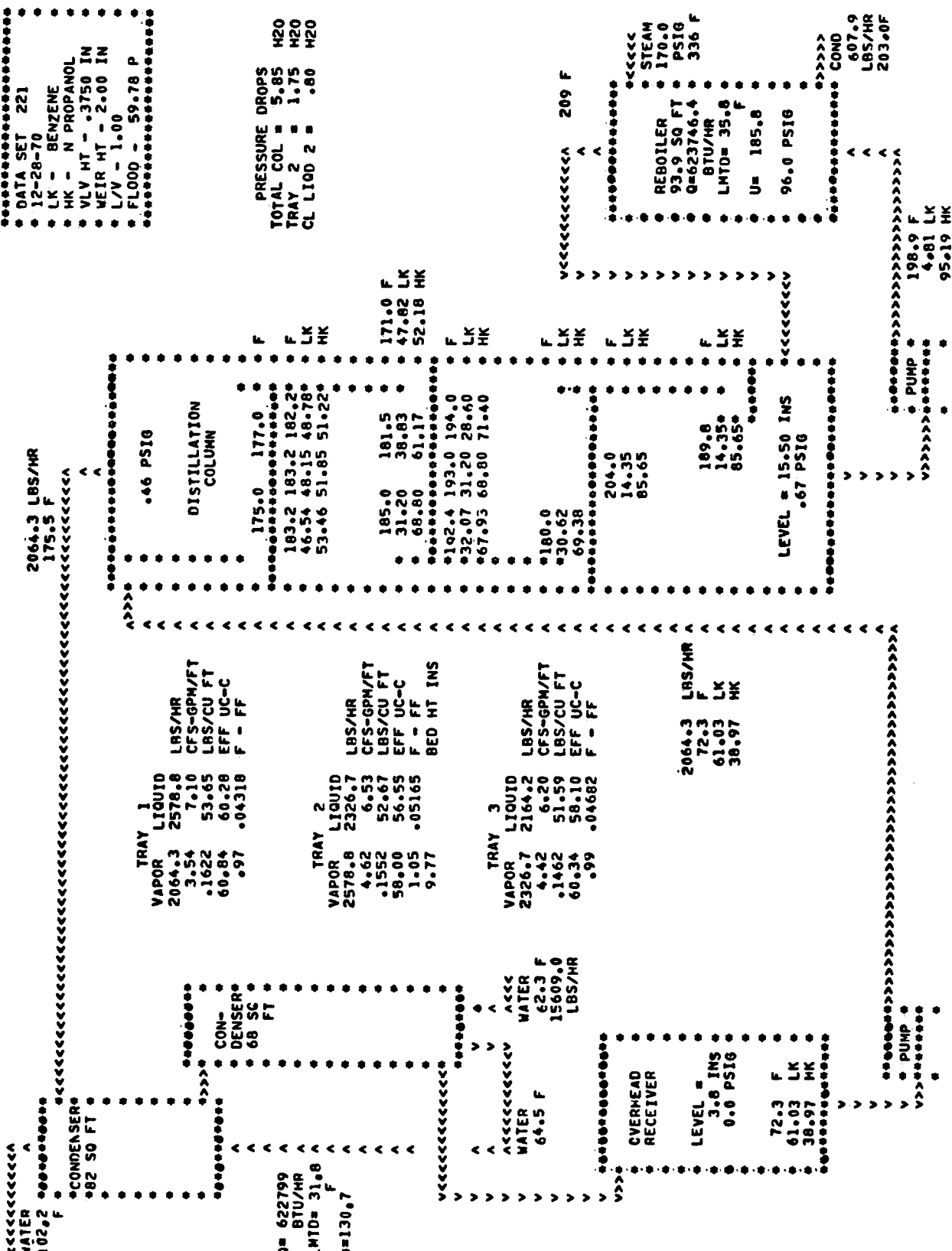


Figure 9. Experimental data analysis

column efficiency. This same conclusion has been made by other studies (A.I.Ch.E., 1958; Finch, 1964; Kocatas, 1962; Umholtz, 1957).

The tabulated data of Table V show a slight negative effect of the tray valve leg lengths (increasing the percent free area) on the overall average column efficiency. See Figure 9 for an experimental data analysis.

Accuracy and Reproducibility of Experimental Data

Froth Heights. The precision of the photographic technique for measuring the tray froth heights was determined by calculating the standard deviation about the mean for each set of five froth heights measured. The average of these standard deviations was 0.60 in. This average value is good when the violent motion of the tray bed is considered. The reproducibility of the froth heights was determined by comparing the six duplicate center points of the experimental design (three duplicates for each binary system investigated) and the two duplicate D data sets. The average absolute deviation between the duplicate points was 0.43 in., which is within the accuracy of the photographic technique.

Pressure Measurements. The average absolute deviation between duplicates of the recorded clear liquid heights was calculated to be 0.07 in. for the six duplicate center points and the duplicate D, E, and F data sets. When these same data points were used, the average absolute deviation between duplicates of the measured tray pressure drops was computed to be 0.08 in. These average deviations are within the accuracy of the recording instruments.

Efficiencies. Again using the six center design duplicate points and the duplicate D, E, and F data sets, the average absolute deviation between the duplicates of the Murphree test tray efficiencies was calculated to be 1.49%. The reproducibility of the efficiency data for the second tray was dependent upon the stability of the distillation column operation. Normally the operations at the extremes of the operating range of the column (15 and 98% of column flood) were the least stable. If these points are not considered, the average absolute deviation between the duplicate data points decreases to 1.07%. The average column efficiency data demonstrated a higher degree of reproducibility than the data of the second tray and had an average absolute deviation between duplicate points of 0.70%.

Conclusions

The experimental results show that the tray efficiencies for the *n*-propanol-toluene binary system were definitely higher than the corresponding tray efficiencies of the benzene-*n*-propanol binary system. Visual observations of the operating tray could not account for these variances in efficiencies and it is therefore concluded that the variances must be the result of some basic difference in the heat and mass transfer mechanisms occurring between the distilling phases. It was also concluded that vaporization in the downcomers (see the Appendix) increases the Murphree tray efficiency. From visual observation, this type of valve tray exhibited a surprisingly small amount of tray weepage at low flow rates.

This study demonstrates that valid efficiency, pressure drop, and froth height data can be obtained from a small pilot size distillation column containing a minimum number of trays.

Acknowledgment

The authors wish to express their appreciation to the National Science Foundation, Southwestern Oil and Refining Co., Nutter Engineering Co., Union Carbide Co., and Monsanto Chemical Co.

APPENDIX

Experimental Data

The tabulated experimental results were prepared from the raw experimental data by the following procedures:

1. The overhead, bottom, reflux, cooling water, and steam flow chart readings were computed in units of pounds of water per hour.

2. The weight percent compositions of the samples were computed from the refractive indices and then converted to mole fractions.

3. The pressures of the various internal streams were determined from the column bottom pressure and the total pressure drop across the column.

4. The compositions of the vapors entering and leaving the second tray were assumed to be equal to the average of the three respective vapor samples collected below and above the tray.

5. The equilibrium temperatures for the internal streams were determined by making bubble point calculations on the liquid streams and dew point calculations on the vapor streams. These computed temperatures were assumed to be more accurate than the measured temperatures and were used as the basis for all heat calculations.

6. Using the above compositions, pressures, and temperatures, the enthalpies and densities of each stream were calculated by the procedures recommended by the "A.P.I. Technical Data Book on Refining" (1966).

7. The metered process flows were converted from units of water to units of the flowing material.

8. If the distillation column was functioning as a stripper, the composition and temperature of the stream returning to the top of the column (combined reflux and bottom product streams) were calculated.

9. The internal vapor and liquid flows were computed by making material and enthalpy balances about the bottom section of the column. In performing the following computations, only the vapor sample compositions were used. The balances resulted in the following equations:

$$V_n + B = L_{n-1} + D \quad (1)$$

$$V_n H_n + B h_B = L_{n-1} h_{n-1} + D h_D + Q_R - Q_D \quad (2)$$

Q_D was defined as the amount of heat conducted through the downcomer wall and was computed by the following equation.

$$Q_D = UA\Delta T \quad (3)$$

where

$$U = 200 \text{ Btu/ft}^2 \text{ hr, } ^\circ\text{F}$$

$$A = 2.71 \text{ ft}^2$$

$$\Delta T = T_{L_{n-1}} - T_{V_n}$$

Solving for V_n results in the following equation:

$$V_n = \frac{Q_R - Q_D + D(h_D - h_{n-1}) + B(h_{n-1} - h_B)}{H_n - h_{n-1}} \quad (4)$$

Therefore, V_n can be computed if the value of h_{n-1} is known. The value of the liquid composition of L_{n-1} was assumed

and h_{n-1} was calculated. The value of V_n was then calculated from the above equation and the assumed value of x_{n-1} checked by the following equation:

$$x_{n-1} = \frac{x_n V_n + x_B B - x_D D}{L_{n-1}} \quad (5)$$

The new value for x_{n-1} was then used to recompute V_n . This procedure was repeated until the difference in values of x_{n-1} between successive iterations was less than 0.0001.

10. The Murphree tray efficiencies were computed from the experimental vapor compositions by the following equation:

$$E_{MV} = \frac{y_n - y_{n+1}}{mx_n - y_{n+1}} \quad (6)$$

11. The liquid compositions were corrected for possible vaporization of the liquid in the downcomer. This was done by estimating the quantity of liquid vaporized in the downcomer by the following material and enthalpy balances:

$$L_n^* = V_n^* + L_n \quad (7)$$

where

V_n^* = moles of vapor formed in downcomer, mol/hr

L_n^* = moles of liquid entering downcomer, mol/hr

L_n = moles of liquid leaving downcomer, mol/hr

$$V_n^* = \frac{Q_D + L_n(h_n^* - h_n)}{H_n^* - h_n} \quad (8)$$

V_n^* was assumed initially to be in equilibrium with L_n to permit the calculation of H_n^* , and the difference $h_n^* - h_n$ was assumed to be equal to zero. The value of V_n^* was then calculated from the above equation. x_n^* was then determined by the following relationship:

$$x_n^* = \frac{y_n^* V_n^* + x_n L_n}{L_n^*} \quad (9)$$

A bubble point calculation on x_n^* determined the temperature of the entering liquid and h_n^* was then computed and V_n^* was recalculated. This procedure was repeated until the assumed value of V_n^* converged to a constant value.

12. The vapor compositions were corrected to account for the vapor generated in the downcomers by the following relationship:

$$y_n' = \frac{y_n V_n - y_n^* V_n^*}{V_n - V_n^*} \quad (10)$$

The equation for computing the efficiency then becomes

$$E_{MV}^c = \frac{y_n' - y_{n+1}'}{mx_n^* - y_{n+1}'} \quad (11)$$

The values of the corrected efficiencies were always less than the values of the uncorrected efficiencies; therefore, it was concluded that vaporization in the downcomers increases the efficiency of a distillation tray. Both the corrected and uncorrected efficiencies are reported for each tray in the tabulated data.

13. The F_s -factors and the frothing factor were computed for each tray by using the appropriate average values of the entering and exiting streams. The column cross-sectional area (1.68 ft^2) was used in computing the F_s -factor, and the active or bubbling area (1.06 ft^2) was used in computing the frothing factors. The liquid flow per length of outlet weir was computed by using the quantity of liquid leaving the tray. A weir length of 0.844 ft was used in the computations.

14. The heat duties, log mean temperature differences, and

overall heat transfer coefficients for the condenser and reboiler were computed by standard equations.

In the tabulated data of Figure 9, LK and HK represent the compositions of the two components expressed as mole percent. The symbol F is used to represent both the F_s -factor of the tray data and the temperatures of the various streams in degrees Fahrenheit. The letters UC and C denote the respective uncorrected and corrected tray efficiencies.

Nomenclature

A_a = active or bubbling area of valve tray, ft^2

B = bottom product flow, lb mol/hr

D = overhead product flow, lb mol/hr

E_{MV} = Murphree tray efficiency in vapor terms

E_{MV}^c = Murphree tray efficiency in vapor terms, corrected for heat transfer through downcomer walls

\overline{E}_{MV}^c = average column corrected Murphree tray efficiency in vapor terms

F_s = $U_s(\rho_v)^{0.5} = F_s$ -factor (ft/sec) (lb/ft^3) $^{1/2}$

FF = $U_a^2 \rho_v / (\rho_L - \rho_v) = FF$, average frothing factor

h = liquid enthalpy, Btu/lb mol

H = vapor enthalpy, Btu/lb mol

L = liquid flow, lb mol/hr

m = vapor-liquid equilibrium constant

ΔP_T = pressure drop across tray 2, in. H_2O

Q_D = heat conducted through walls of downcomer, Btu/hr

Q_R = heat input to reboiler, Btu/hr

T = temperature, °F

V = vapor flow, lb mol/hr

x = liquid composition, mole fraction

y = vapor composition, mole fraction

Z_c = clear liquid height, in.

Z_f = froth height, in.

SUBSCRIPTS

n = tray n

Literature Cited

- A.I.Ch.E., "Tray Efficiencies in Distillation Columns," Final Report from University of Delaware to A.I.Ch.E. Research Committee, 1958.
- Box, G. E. P., Behnken, D. W., *Technometrics*, **2**, 455-75 (1960).
- Dale, G. H., Dove, W. T., Huntington, R. L., *Hydrocarbon Process.*, **41**, 117-20 (1962).
- Ellis, S. R., Shelton, J. T., "Interstage Heat Transfer and Plate Efficiency in a Bubble-Plate Column," International Symposium on Distillation, Institution of Chem. Engr., London, May 1960, pp 171-6.
- Finch, R. M., Van Winkle, M., *Ind. Eng. Chem. Process Des. Develop.*, **3**, 106-16 (1964).
- Flint, E., "Foaming in Small Perforated Plate Distillation Columns," Master's Thesis, The University of Texas, January 1965.
- Fractionation Research, Inc., "Report of Test of Nutter Type B Float Valve Trays," Alhambra, Calif., July 2, 1964.
- Gerster, J. A., Bonnett, W. E., Hess, Irwin, *Chem. Eng. Progr.*, **47**, 523, 621 (1951).
- Hellums, J. D., Braulick, C. J., Lyda, C. D., Van Winkle, M., *AICHE J.*, **4**, 465 (1958).
- Koch News, Wichita, Kan., July 1, 1958.
- Kocatus, B. M., "Evaluation of Sieve Tray Distillation Column by Statistically Designed Experiments," PhD dissertation, University of Texas, 1962.
- Lowry, R., "Foaming and Frothing Related to System Physical Properties in a Small Perforated Plate Distillation Column," PhD Dissertation, University of Texas, June 1967.
- Lu, B. C. Y., *Can. J. Technol.*, **34**, 468-72 (1957).
- Prabhu, P. S., Van Winkle, M., *J. Chem. Eng. Data*, **8**, 210-14 (1963).
- Sawistowski, H., Smith, W., *Ind. Eng. Chem.*, **51**, 915-18 (1959).
- "Technical Data Book—Petroleum Refining," Amer. Petrol. Inst., Division of Refining, New York, N.Y., 1966.
- Todd, W. G., Van Winkle, M., *Ind. Eng. Chem. Process Des. Develop.*, **6**, 95-101 (1967).
- Umholtz, C. L., Jones, P. D., Van Winkle, M., *Ind. Eng. Chem.*, **49**, 226 (1957).

RECEIVED for review March 13, 1972

ACCEPTED June 5, 1972